Investigation of Peroxidase-Like Activity of Flower-Shaped Nanobiocatalyst from *Viburnum Opulus L.* Extract on the Polymerization Reactions

Berkant Kalayci¹ (iD), **Naime Kaplan²** (iD), **Muge Mirioglu¹** (iD), **Seyma Dadi³** (iD), **Ismail Ocsoy⁴** (iD), **Ersen Gokturk¹*** (iD)

¹Department of Chemistry, Hatay Mustafa Kemal University, Hatay, 31001, Turkey.
²Department of Chemistry, Gaziantep University, Gaziantep, 27310, Turkey.
³Department of Nanotechnology Engineering, Abdullah Gül University, Kayseri, 38080, Turkey.
⁴Department of Analytical Chemistry, Faculty of Pharmacy, Erciyes University, Kayseri, 38039, Turkey.

Abstract: Here, we report the effects of peroxidase-mimicking activity of flower shaped hybrid nanobiocatalyst obtained from *Viburnum-Opulus L.* (Gilaburu) extract and Cu^{2+} ions on the polymerization of phenol and its derivatives (guaiacol and salicylic acid). The obtained nanoflowers exhibited quite high catalytic activity upon the polymerization of phenol and guaiacol. The yields and the number average molecular weights of the obtained polymers were significantly high. Due to solubility issue of salicylic acid in aqueous media, polymerization of salicylic acid resulted in very low yields. Free-horseradish peroxidase (HRP) enzyme is known to be losing its catalytic activity at 60 °C and above temperatures. However, the synthesized nanoflowers exhibited quite high catalytic activity even at 60 °C and above reaction temperatures. This provides notable benefits for reactions needed at high temperatures, and it is very important to use these kinds of nanobiocatalysts for both scientific studies and industrial applications.

1. INTRODUCTION

Enzyme catalyzed polymerization reactions have been extensively studied due to being environmentally benign and simple procedure for different purposes (1,2). Peroxidase enzymes oxidize proton donor compound using hydrogen peroxide (H_2O_2), and two moles of water are released. Peroxidases, such as horseradish peroxidase (HRP) and soybean peroxidase (SBP), typically consist of iron (Fe) ions in their active centers (3). These centers initiate radical polymerization reactions of vinyl monomers and some aromatic compounds, including phenol, aniline, etc (4).

Dordick and coworkers were the first group reporting the enzymatic polymerization of phenol (5). A variety of organic and inorganic electron donating compounds, including phenols, amines, indoles, phenolic acids, and sulfates, could be oxidized by peroxidase enzymes (6,7). Therefore, different kinds of polymers could be manufactured in good yields. Even though the enzymatic polymerization method is known to be environmentally benign and simple procedure for different studies, there are some limitations to use enzymes in industrial scale applications. In addition to the high cost of enzymes, their instability and decreased catalytic activity in aqueous solutions are known to be important drawbacks for enzymatic polymerization reactions (8,9). Immobilization of enzymes is applied to solve these drawbacks and has been partially successful. Enzyme immobilization increases the stability of enzymes and makes them reusable (1). However, most enzymes lose their catalytic activity after immobilization due to inappropriate conformation and mass transfer limitations between enzyme and substrate (10,11). Because of this reason, it is very

important to apply a suitable immobilization technique in order to use enzymes efficiently in many applications or to discover new generation catalysts that can show similar catalytic activities as enzymes.

Hybrid organic-inorganic flower shaped nanobiocatalysts were first reported by Ge and coworkers (12). Different proteins as organic sources and Cu(II) ions as inorganic constituent were used to generate hybrid nanoflowers. Complexation between protein and Cu^{2+} ions generated flower-shaped micrometer-sized particles. Even though these particles were micrometer-sized, they were named nanoflowers because of their nanoscale properties. The obtained protein-Cu^{2+} nanoflowers showed very high catalytic activity and stability. These nanoflowers showed 2.5 times higher catalytic activity compared to the free laccase enzyme on the oxidation of epinephrine. While free-laccase enzyme lost 50% of its catalytic activity within 10 days, the nanoflowers showed higher than 95% of catalytic activity even after 2 months. There are limited numbers of studies in the literature related to the utilization of hybrid nanoflowers in polymerization studies. Gokturk and coworkers synthesized flower shaped hybrid HRP-Cu^{2+} nanoflowers from free-HRP enzyme and Cu^{2+} ions (13). Obtained HRP-Cu^{2+} nanoflowers exhibited quite high catalytic activity and stability towards polymerization of hydroquinone, catechol, and resorcinol. Up to 95% of polymerization yield was observed. The nanoflowers also showed very good catalytic activity even at 60 °C reaction temperature without denaturation. Another interesting study about the formation of hybrid nanoflowers and their applications in the polymer synthesis was also reported by Gokturk and coworkers. In this study, the complexation between green tea extract as an organic component and Cu^{2+} ions as an inorganic component was accomplished, and flower shaped green tea-Cu^{2+} nanobiocatalyst was observed (4). Obtained green tea-Cu^{2+} nanoflowers exhibited peroxidase-mimicking activity towards polymerization of phenol derivatives. Polymerization of phenol using green tea-Cu^{2+} nanoflowers was achieved at 60 °C reaction temperature with 82% of yield. Green tea-Cu^{2+} nanoflowers also showed very good catalytic activity and stability up to 60 °C reaction temperature in which free-HRP enzyme denatures.

In this study, the effects of peroxidase-mimicking activity of hybrid nanobiocatalyst obtained from *Viburnum-Opulus L.* (Vib.-Op. L.) extract and Cu^{2+} ions on the polymerization of phenol and its derivatives (guaiacol and salicylic acid) were investigated. The obtained nanoflowers exhibited quite high catalytic activity upon the polymerization of phenol and guaiacol. The yields and the number average molecular weights of the obtained polymers were significantly high. Due to the solubility issue of salicylic acid in aqueous media, polymerization of salicylic acid resulted in very low yields. Even though free-HRP enzyme starts losing its catalytic activity at 60 °C, the synthesized nanoflowers exhibited quite high catalytic activity even at 60 °C and above reaction temperatures. This provides notable

benefits for reactions needed at high temperatures, and is very important to use these nanoflowers for both scientific and industrial applications.

2. EXPERIMENTAL SECTION

2.1. Instrumentation
Bruker-Instruments-NMR (DPX-400) 400 MHz spectrometer was used for the ^1H and ^{13}C nuclear magnetic resonance (^1H and ^{13}C NMR) spectra of the products. Scanning electron microscope (SEM) images were monitored using Zeiss Gemini 500 instrument. Shimadzu IRAffinity-1S spectrometer was utilized for FT-IR analyses of the products. Thermogravimetric analyses were carried out with a Mettler-Toledo TGA/DSC 1 Star system instrument under nitrogen (N_2) at 10 °C/min heating rate from room temperature (RT) to 1000 °C. Differential scanning calorimetry (DSC) analyses were performed with a Mettler-Toledo DSC 1 Star system instrument with a heat cycle at 10 °C/min from 0 °C to 500 °C under N_2. Shimadzu LC-20AD instrument was used for the gel permeation chromatography (GPC) analyses of the polymers at 40 °C using HPLC grade N,N`-dimethylformamide (DMF) mobile phase at 1 mL/min flow rate. Narrow polydispersity polystyrene (PS) standards were used for the calibration. TGA, DSC, and GPC analyses results were given in supporting information.

2.2. Extraction of Vib.-Op. L.
20 g of dry Vib.-Op. L. fruits (gilaburu) were powdered by porcelain mortar and pestle. It was then extracted in 200 mL of methanol at RT for 3 days. Collected extract was first filtered (Whatman filter paper# 1, pore size 25 μm), and then solvent was evaporated. The dried extract was kept in the refrigerator at +4 °C for nanobiocatalyst production (14).

2.3. Synthesis of Vib.-Op.-Cu^{2+} Nanoflowers
Viburnum Opulus L. extract at a concentration of 0.1 mg/mL was poured into 50 mL of a mixture consisting of 10 mM pH 7.4 PBS buffer and 0.8 mM $CuSO_4.5H_2O$ (copper sulfate pentahydrate). The resulting solution was vortexed and kept in the refrigerator at +4 °C for 3 days. The mixture was then centrifuged to collect blue-colored precipitate and washed with water 3 times to eliminate impurities. The blue solid product was then dried and kept in the refrigerator at +4 °C for polymerizations (14).

2.4. Representative Polymerization Procedure
100 mg of phenol derivative monomers (phenol, guaiacol, and salicylic acid) and the nanoflowers were put in 5.0 mL of buffer solution. In order to ensure solubility in the polymerization of salicylic acid, 0.2 mL of THF was also added to the mixture. The reaction was adjusted to the desired temperature. Then, polymerization was initiated by adding 70 μL of hydrogen peroxide (H_2O_2) to the mixture at 10 minutes intervals for 15 times. At the end of polymerization, the black precipitate was centrifuged, washed with water and methanol, and dried. The optimum polymerization condition was determined by performing the polymerization

reactions at different pH (pH: 7.0, 7.4, and 8.0), with different weight percentages (7.5, 10.0, and 15.0%) of catalyst loadings and at different temperatures (40, 50, 60, and 70 °C) (13).

FT-IR (ATR) spectrum of polyphenol (entry 7 in Table 1): 3400 cm^{-1} (O–H stretch), 1720 cm^{-1} and 1620 cm^{-1} (C=C aromatic stretch), 1195 cm^{-1} (C–O), 950 cm^{-1}, 650 cm^{-1}. ^{1}H NMR spectrum of polyphenol (entry 7 in Table 1) (400 MHz, DMSO-d_6, δ, ppm): 6.67-6.70 (5H, m, Ar-*H*). ^{13}C NMR spectrum of polyphenol (100 MHz, DMSO-d_6): δ 145.7 (Ar-*O*), 129.8, 119.7, 116.1, 100.0 (Ar-*C*H).

FT-IR (ATR) spectrum of polyguaiacol (entry 9 in Table 1): 3500 cm^{-1} (O–H stretch), 1712 cm^{-1} and 1604 cm^{-1} (C=C aromatic stretch), 1195 cm^{-1} (C–O), 817 cm^{-1}, 763 cm^{-1}. ^{1}H NMR spectrum of polyguaiacol (entry 9 in Table 1) (400 MHz, DMSO-d_6, δ, ppm): 6.84 (4H, m, Ar-*H*), 3.75 (3H, s, OC*H*$_3$). ^{13}C NMR spectrum of polyguaiacol (100 MHz, DMSO-d_6): δ 145.6 (Ar-*O*), 119.8, 116.1, 100.0 (Ar-*C*H), 56.4 (O*C*H$_3$).

FT-IR (ATR) spectrum of polysalicylic acid (entry 10 in Table 1): 3500 cm^{-1} (O–H stretch), 1705 cm^{-1} (C=O), 1160 cm^{-1} (C–O), 816 cm^{-1}, 964 cm^{-1}. ^{1}H NMR spectrum of polysalicylic acid (entry 10 in Table 1) (400 MHz, DMSO-d_6, δ, ppm): 12.48 (1H, s, COOH), 6.55-8.65 (4H, m, Ar-*H*). ^{13}C NMR spectrum of polysalicylic acid (100 MHz, DMSO-d_6): δ 161.6 (*C*OOH), 135.9 (Ar-*O*), 130.7, 119.5, 117.4, 100.0 (Ar-*C*H).

3. RESULTS AND DISCUSSION

Scanning electron microscope (SEM) images of the Vib.-Op.-Cu^{2+} nanoflowers obtained from the complexation between *Viburnum-Opulus L.* extract and Cu^{2+} ions were illustrated in Figure 1. The Vib.-Op.-Cu^{2+} nanobiocatalyst has a spherical morphology and snowball appearances just like *Viburnum Opulus L.* flower seen on the right corner of Figure 1a. The average diameter of flower shaped spheres was found to be approximately 10 μm, and these flowers showed narrow size distributions. Although the size of the obtained Vib.-Op.-Cu^{2+} particles are micrometer-scale, these flowers are named nanobiocatalysts because they show nanoscale characteristics as mentioned in the literature (12).
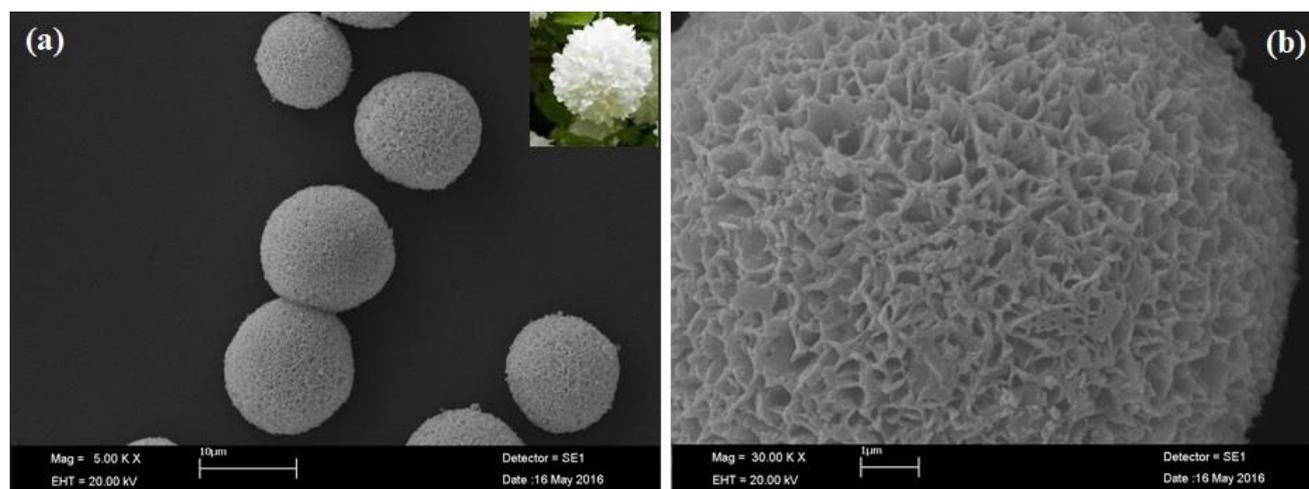
Figure 1: The spherical morphology of Vib.-Op.-Cu^{2+} nanoflowers.

The results of the polymerization of phenol derivatives in the presence of hybrid nanoflowers (Vib.-Op.-Cu^{2+}) are given in Table 1. The reaction temperature, solution pH, and catalyst amount were first optimized in the polymerization of phenol using Vib.-Op.-Cu^{2+} nanoflowers (Figure 2). All polymerizations were performed in buffer media. In order to examine the influence of solution pH on the polymerization of phenol, three different buffer solutions (pH: 7.0, 7.4, and 8.0) were used in the reactions. The results showed that polymerizations performed in pH 7.4 buffer at 50 °C (Table 1, entry 1) resulted in the highest yield and molecular weight of the polyphenol compared to the other buffers. Polymerizations in pH 7.0 (Table 1, entry 4) and pH 8.0 (Table 1, entry 5) buffers also showed high yields, but both yields and molecular weights of the polymers were lower than the product obtained at pH 7.4.
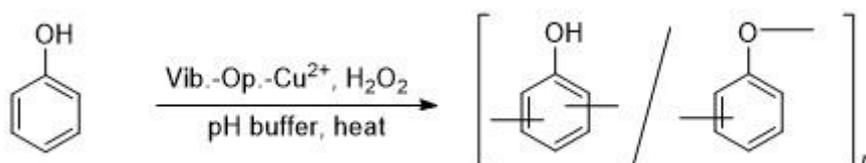
Figure 2: Polymerization of phenol using hybrid Vib.-Op.-Cu^{2+} nanoflowers in the presence of H$_2$O$_2$.

In order to optimize the amount of nanoflowers, polymerization of phenol was accomplished with three different catalyst loadings: 7.5 wt% (Table 1, entry 1), 10 wt% (Table 1, entry 2), and 15 wt% (Table 1, entry 3) at 50 °C in pH 7.4 buffer. The highest polymer yield was 78% obtained with 15 wt% of catalyst loading relative to phenol (Table 1, entry 3). The polymerization yield with 7.5 wt% of catalyst loading was 74%, which is slightly lower than that of 15 wt% of catalyst loading. However, thermal stability and the average molecular weight of the obtained polymer with 7.5 wt% of catalyst loading were considerably higher than that of the polymer obtained with 15 wt% of catalyst loading. Due to the observation of better thermal properties and higher molecular weight, the optimum amount of catalyst loading for the polymerization of phenol was determined to be 7.5 wt%.

Table 1: Polymerization of phenol and its derivatives by Vib.-Op.-Cu^{2+} nanoflowers in the presence of H_2O_2.

Entry	Weight% Vib.-Op.-Cu^{2+}	pH	T_p (°C)	Yield (%)	T_{50} (°C)	Residue (%) at 1000 °C	M_n (Da)	Đ
1[a]	7.5	7.4	50	74	630	23.8	122000	2.86
2[a]	10.0	7.4	50	76	540	18.0	104000	2.75
3[a]	15.0	7.4	50	78	489	2.7	77000	3.43
4[a]	7.5	7.0	50	73	614	18.6	71000	2.99
5[a]	7.5	8.0	50	67	450	2.6	66000	2.75
6[a]	7.5	7.4	40	61	477	7.2	80000	3.23
7[a]	7.5	7.4	60	81	620	29.1	202000	2.26
8[a]	7.5	7.4	70	74	612	28.8	118000	3.25
9[b]	7.5	7.4	60	37	628	28.9	90000	3.02
10[c]	7.5	7.4	60	10	431	2.0	49000	3.13

[a]100 mg of phenol in different pH buffers were polymerized in the presence of H_2O_2, [b]100 mg of guaiacol was polymerized in the presence of H_2O_2, [c]100 mg of salicylic acid was polymerized in the mixture of 4.8 mL of pH 7.4 buffer and 0.2 mL of THF in the presence of H_2O_2, T_p= reaction temperature, T_{50}= temperature at 50% residue, M_n: the number average molecular weight, Đ: polydispersity index (M_n and Đ values for the polymers were given in supporting information).

The influence of reaction temperature on the polymerization yield and the number average molecular weights of the synthesized polymers were also examined as the last optimization parameter. Four different temperatures between 40 °C and 70 °C were tried to detect the optimum polymerization temperature. The highest yield was accomplished at 60 °C (Table 1, entry 7). HRP enzyme is known to denature and lose its catalytic activity at 60 °C and above temperatures (15). Obtained successful outcomes indicated that Vib.-Op.-Cu^{2+} nanoflowers showed very high catalytic activity even at 70 °C reaction temperature (Table 1, entry 8), and provided 74% of polymer yield. This suggests that Vib.-Op.-Cu^{2+} nanoflowers can be used for some radical polymerization reactions requiring high temperatures. All these optimization parameters for the polymerization of phenol using Vib.-Op.-Cu^{2+} catalyst showed that 7.5 wt% catalyst loading in pH 7.4 buffer at 60 °C reaction temperature (entry 7 in Table 1) resulted in 81% of yield, and the molecular weight of the polyphenol was 202000 Da. In the literature, free-HRP enzyme catalyzed polymerization of phenol was isolated up to 95% of yield under pH 6.9 buffer at RT (16). According to our findings, Vib.-Op.-Cu^{2+} nanoflowers showed lower catalytic activity towards polymerization of phenol compared to the free-HRP enzyme. However, lower cost and showing very high stability at high reaction temperatures are noticeable properties of Vib.-Op.-Cu^{2+} nanoflowers compared with HRP enzyme. Thermal analysis results of this polymer under nitrogen (N_2) atmosphere showed that polyphenol lost 50% of its weight at 620 °C, and carbonaceous residue at 1000 °C was 29% (Figure S7, supplementary information). The polydispersity index was found to be 2.26, and this shows that polyphenol has partially narrow molecular weight distribution. Differential scanning calorimetry (DSC) analysis of polymer 7 (entry 7 in Table 1) is shown in Figure S11 (supplementary information). A broad peak was observed at 110 °C due to the thermosetting property of the polyphenol (13). Carbon-oxygen (oxy-ortho or oxy-para) and carbon-carbon (ortho-ortho or ortho-para) couplings occur during the polymerization of phenol, and therefore, cross-linking properties could be observed due to these couplings in the polymer repeating units.

FT-IR, ^{1}H and ^{13}C NMR analyses were carried out for the structural characterizations of the obtained polymers. According to the FT-IR spectrum of the polyphenol obtained from entry 7 in Table 1, the broad band detected around 3400 cm^{-1} belongs to the hydroxyl (-OH) stretching vibration (Figure 3a). The peaks observed around 1720 and 1620 cm^{-1} indicate aromatic (-C=C-) stretching vibrations. The C-O absorption band is observed at 1195 cm^{-1} (17). The vibration bands observed at 650 and 950 cm^{-1} indicate 1,2 and 1,4 substitutions occurred in the polyphenol structure, proving that polymerization takes place at *ortho*- and *para*- positions of phenol (18).
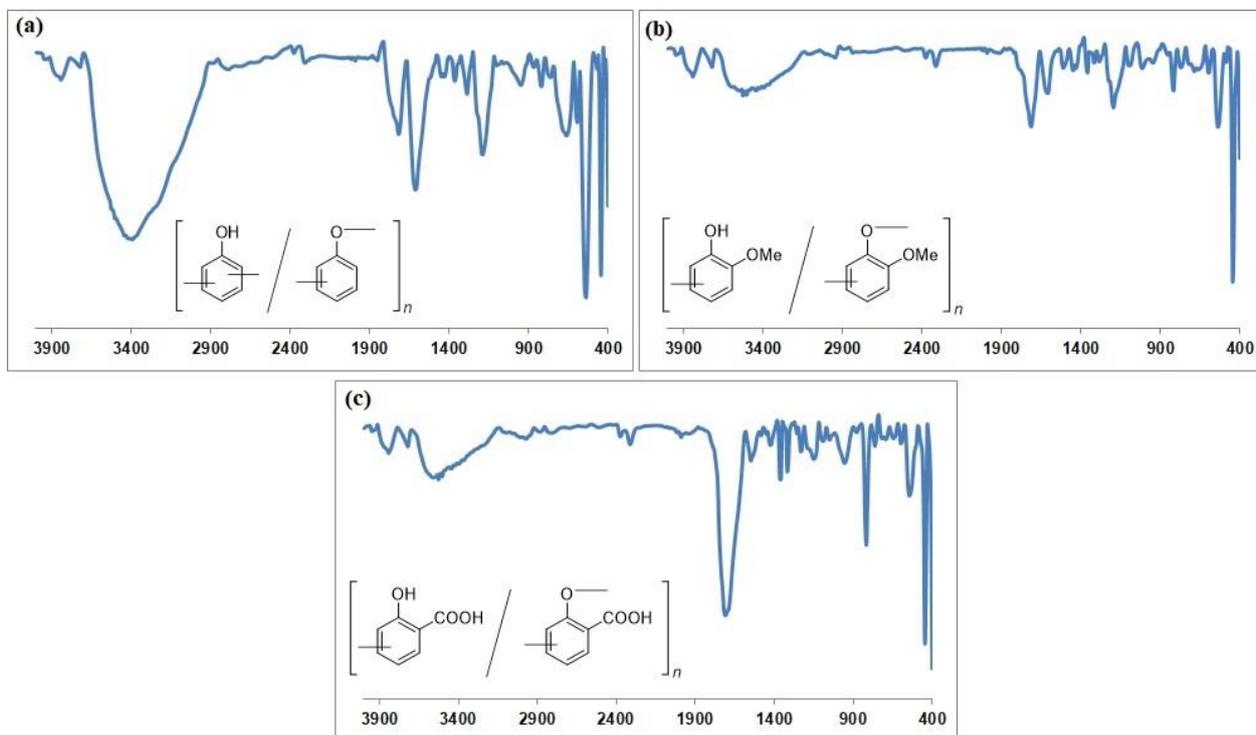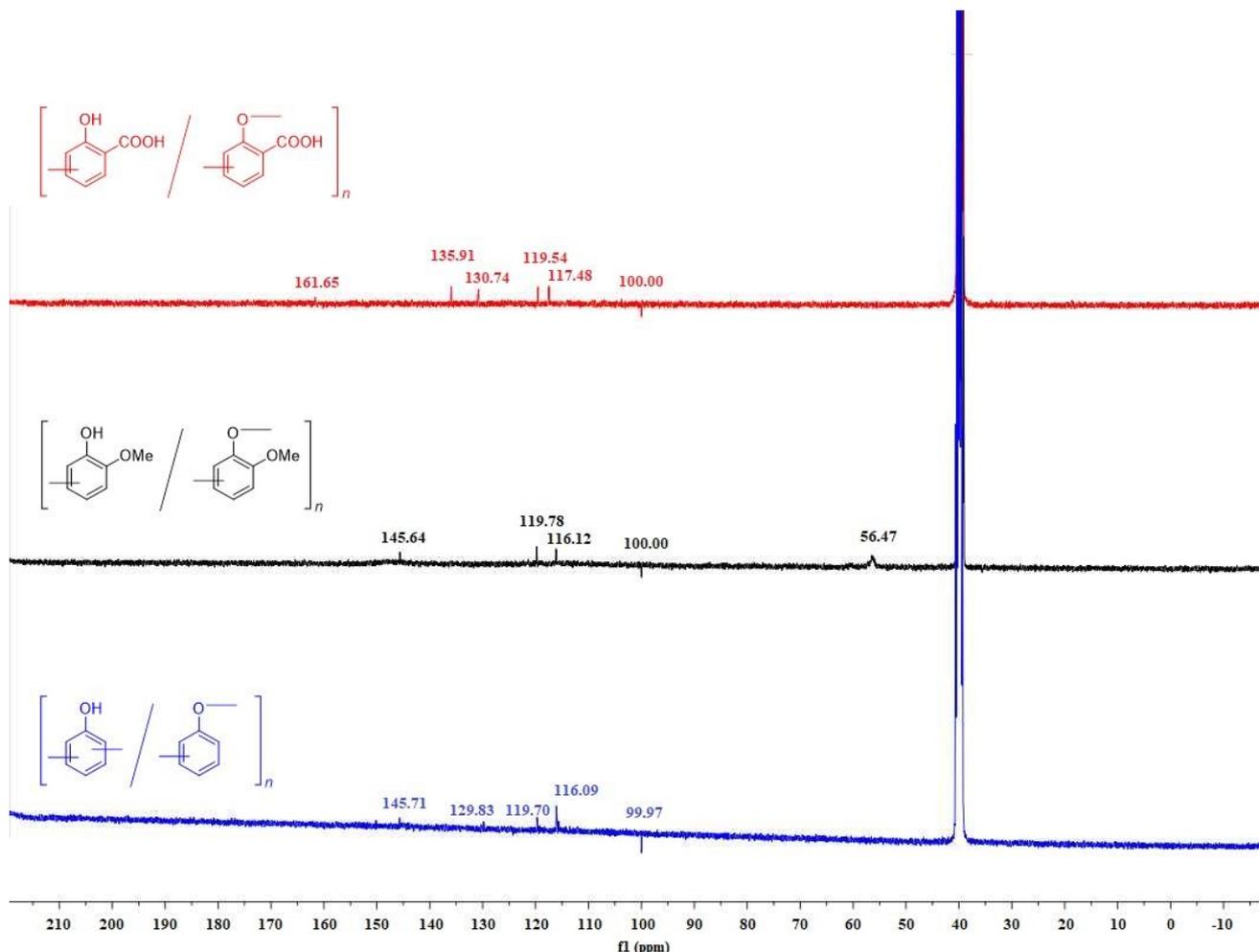
Figure 3: FT-IR spectra results of (a) polyphenol (entry 7 in Table 1), (b) polyguaiacol (entry 9 in Table 1), (c) polysalicylic acid (entry 10 in Table 1).
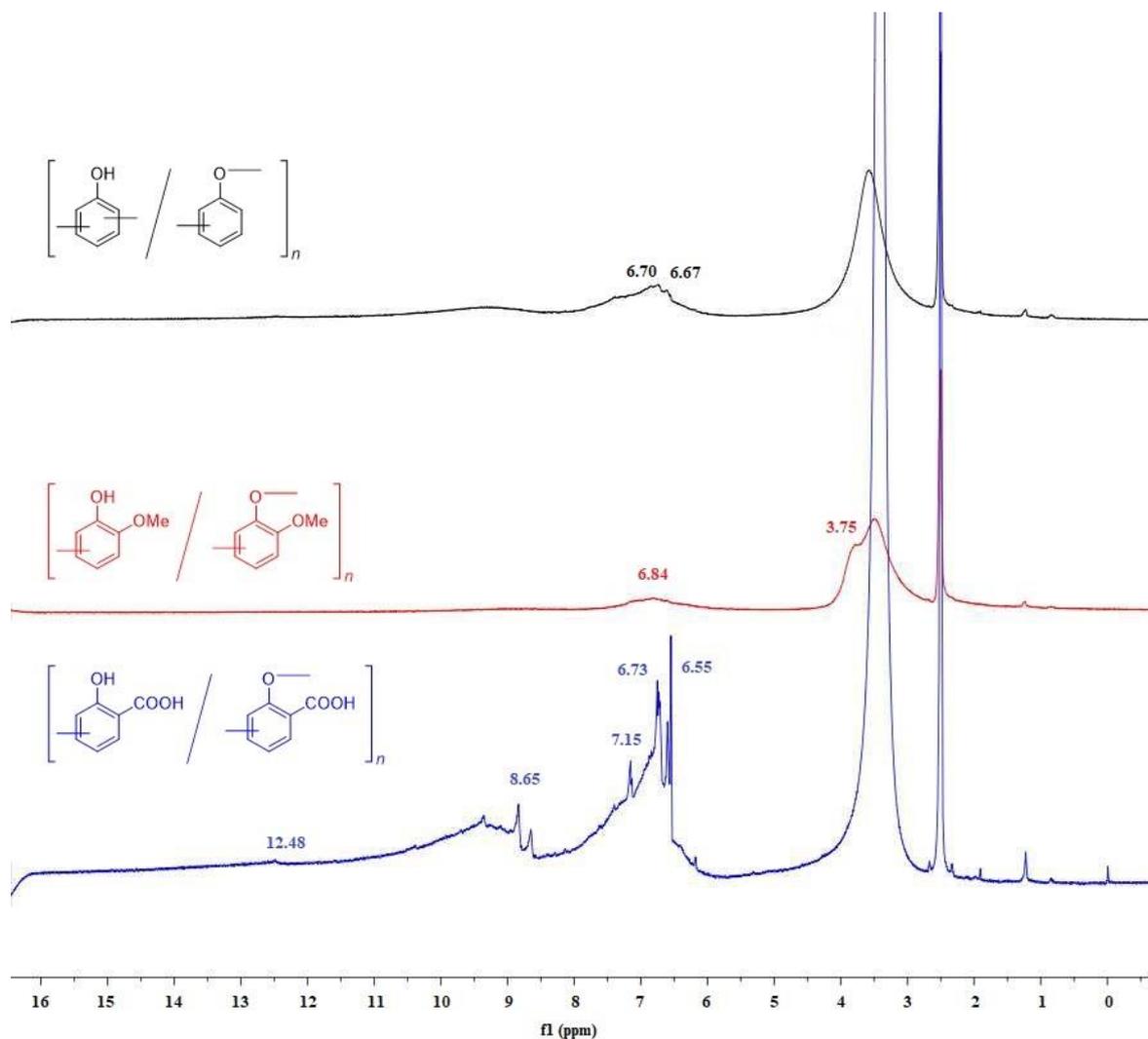
Figure 4: ^{1}H NMR spectra results of polyphenol (top, entry 7 in Table 1), polyguaiacol (middle, entry 9 in Table 1), polysalicylic acid (bottom, entry 10 in Table 1).

In addition to the FT-IR results, ^{1}H and ^{13}C NMR analyses were also performed to verify the structure of the obtained polymer. ^{1}H NMR spectrum of polymer 7 (entry 7 in Table 1) showed only aromatic protons due to the polyphenol structure (Figure 4). The broad peak observed between 6.67 ppm and 6.70 ppm belongs to aromatic C-H protons. The broadening of the peaks observed in the spectrum is due to the formation of polymeric structure. Phenolic hydroxyl (-OH) proton was not observed in the ^{1}H NMR spectrum. Presumably, the hydroxyl (-OH) peak

cannot be seen due to the polymerization proceeding through oxy-phenylene couplings from the phenolic hydroxyl (-OH) group. In addition to that, exchange of hydrogen and deuterium atoms in the DMSO-d_6 NMR solvent of the polyphenol sample might be the reason for this observation (13). ^{13}C NMR spectrum of polymer 7 (entry 7 in Table 1) also confirms the ^{1}H NMR spectrum. The peaks detected in the aromatic region between 100.0-145.7 ppm proved the presence of aromatic carbons in the structure (Figure 5).


Figure 5: ^{13}C NMR spectra results of polyphenol (bottom, entry 7 in Table 1), polyguaiacol (middle, entry 9 in Table 1), polysalicylic acid (top, entry 10 in Table 1).

The optimal reaction condition (entry 7 in Table 1) was also tried for the polymerizations of guaiacol and salicylic acid monomers (Figure 6 and 7). Polymerization of guaiacol using Vib.-Op.-Cu^{2+} nanoflowers resulted in 37% of yield, and the average molecular weight of polyguaiacol was 90000 Da (entry 9 in Table 1). Polydispersity index was 3.02. We previously reported polymerization of guaiacol by free-HRP enzyme in the presence of H_2O_2 in pH 7.4 PBS at 30 °C, and highest polymerization yield was 51% (19). The highest polyguaiacol yield using Vib.-Op.-Cu^{2+} nanoflowers in pH 7.4 at 60 °C was 37%. This result showed that Vib.-Op.-Cu^{2+} nanoflowers demonstrated slightly lower catalytic

activity towards polymerization of guaiacol compared with the free-HRP enzyme. According to the thermal analysis results, the polymer lost 50% of its weight at 628 °C under N_2 atmosphere, and pyrolysis residue of the polymer at 1000 °C was detected to be 28.9% (Figure S9, supplementary information). DSC thermogram of the polyguaiacol (entry 9 in Table 1) is shown in Figure S12 (supplementary information). A broad peak was observed at 110 °C due to the thermosetting property of the polymer. An exothermic broad peak observed at 390 °C is related to the decomposition temperature of polyguaiacol (13).
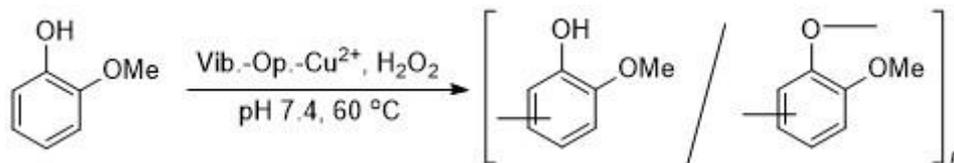
Figure 6: Polymerization of guaiacol using hybrid Vib.-Op.-Cu^{2+} nanoflowers in the presence of H$_2$O$_2$ at 60 °C.
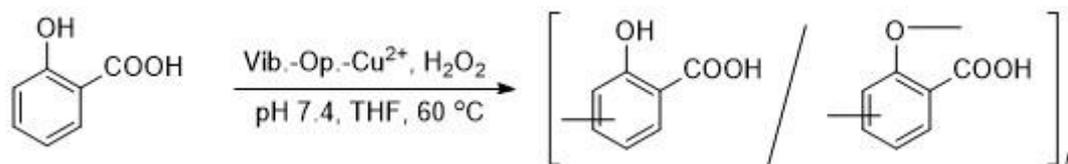
Figure 7: Polymerization of salicylic acid using hybrid Vib.-Op.-Cu^{2+} nanoflowers in 4.8 mL of pH 7.4 buffer and 0.2 mL of THF mixture in the presence of H$_2$O$_2$ at 60 °C.

FT-IR spectrum of the product (entry 9 in Table 1) indicated that an absorption band of hydroxyl (-OH) stretching vibration appeared around 3500 cm^{-1} (Figure 3). The peaks observed at 1712 and 1604 cm^{-1} indicated aromatic (-C=C-) stretching vibrations. C-O absorption band was also observed at 1195 cm^{-1}. Vibration bands at 817 and 763 cm^{-1} show 1,2,4 substitution patterns of the phenyl rings in the polymer repeat units, indicating that polymerization occurred at *ortho*- and *para*- positions of guaiacol.

Figure 4 also shows the ^{1}H NMR spectrum of the product (entry 9 in Table 1). A proton peak appeared at 3.75 ppm as a shoulder can be attributed to methyl group of the methoxy group (-OCH$_3$) in the polyguaiacol structure. Chemical shifts of aromatic protons were observed around 6.84 ppm as a broad peak. Phenolic hydroxyl (-OH) proton in the ^{1}H NMR spectrum of polyguaiacol was not also detected as mentioned in the ^{1}H NMR spectrum of polyphenol (19). ^{13}C NMR spectrum of polymer 9 (entry 9 in Table 1) is illustrated in Figure 5. The existence of the methoxy group (-OCH$_3$) in the polyguaiacol structure was also proved by ^{13}C NMR spectrum. The ^{13}C peak observed at 56.47 ppm indicates the presence of methyl carbon in the methoxy group (-OCH$_3$). The ^{13}C peaks detected between 100.0-145.6 ppm are due to aromatic carbons in the polymer structure.

Entry 7 in Table 1 condition was also applied for the polymerization of salicylic acid (Figure 7). However, salicylic acid was not polymerized due to its insolubility in the buffer solutions. Thus, a small amount of water-soluble organic solvent (tetrahydrofuran, THF) was added into the buffer solution. 4.8 mL of pH 7.4 buffer and 0.2 mL of THF mixture was used in the polymerization of salicylic acid (entry 10 in Table 1). After applying this solvent mixture, 10% of polymer yield was obtained. Increasing the amount of THF resulted in no polymer product, probably due to the decomposition of the nanoflowers in organic solvents (20). Therefore, the optimum amount of THF was determined to be 0.2 mL. The average molecular weight of polysalicylic acid was 49000 Da. Polydispersity index of the polymer was 3.13. 50% mass loss of this polymer

occurred at 431 °C, and the carbonaceous residue at 1000 °C was 2% (Figure S10, supplementary information). According to DSC thermogram of polysalicylic acid (entry 10 in Table 1), a broad peak at 85 °C is attributed to the thermosetting property of the polymer. Exothermic broad peaks observed at 290 °C and 390 °C are related to the decomposition temperatures of the polymer (Figure S13, supplementary information).

Figure 3 also shows FT-IR spectrum of the product (entry 10 in Table 1). Stretching vibration of hydroxyl (-OH) group was observed around 3500 cm^{-1}. Absorption band related to the carbonyl (C=O) group was observed at 1705 cm^{-1}. The C-O vibration band appeared at 1160 cm^{-1}. Peaks detected at 817 and 964 cm^{-1} indicated 1,2,4 substitution patterns of the phenyl ring, indicating that the polymerization occurred at *ortho*- and *para*- positions of phenolic hydroxyl group of salicylic acid. ^{1}H NMR spectrum of polysalicylic acid (entry 10 in Table 1) is also shown in Figure 4. Aromatic protons of polysalicylic acid were observed between 6.50 and 8.65 ppm. A proton detected at 12.48 ppm was attributed to the carboxylic acid proton (-COOH). Figure 5 shows the ^{13}C NMR spectrum of polysalicylic acid (entry 10 in Table 1). The presence of the carbonyl carbon belonging to the carboxylic acid group was also proved by ^{13}C NMR spectrum. ^{13}C peak observed at 161.6 ppm indicates the presence of carbonyl carbon in the carboxylic acid (-COOH) functional group. ^{13}C peaks observed between 100.0-135.9 ppm are due to aromatic carbons in the polymer structure.

4. CONCLUSION

In conclusion, the effects of Vib.-Op.-Cu^{2+} hybrid nanoflowers on the polymerization of phenol derivatives (phenol, guaiacol, and salicylic acid) were investigated. The results showed that hybrid Vib.-Op.-Cu^{2+} nanobiocatalyst demonstrated HRP enzyme-mimicking catalytic activity towards polymerization of phenol derivatives. The yields and the number average molecular weights of the obtained polymers were significantly high. Due to solubility issue of salicylic acid in aqueous media, polymerization of salicylic acid resulted in very low yields. Polymerizations carried out using Vib.-Op.-

Kalayci B et al. JOTCSA. 2024; 11(3): 1321-1328

RESEARCH ARTICLE

Cu^{2+} nanobiocatalyst resulted in very high yields of polymer products without degradation of the catalysts, even at reaction temperatures as high as 60 °C in which peroxidase enzymes can be denatured. This provides notable benefits for reactions needed at high temperatures, and it is very important to use these types of nanoflowers for both scientific studies and industrial applications. Discovery of similar kinds of nanoflowers from proteins (or plant extracts) and metal ions may also expand their utilization in polymer chemistry as promising catalytic reagents for radical polymerizations. Future studies will focus on understanding the origin of catalytic activity of Vib.-Op.-Cu^{2+} nanoflowers, and similar kinds of nanostructures will be tried to synthesize from the isolated active components of *Viburnum Opulus L.* extract.

5. CONFLICT OF INTEREST

The authors have no conflicts of interest to declare.

6. ACKNOWLEDGMENTS

7. REFERENCES

1. Altinkaynak C, Tavlasoglu S, ÿzdemir N, Ocsoy I. A new generation approach in enzyme immobilization: Organic-inorganic hybrid nanoflowers with enhanced catalytic activity and stability. Enzyme Microb Technol [Internet]. 2016 Nov;93–94:105–12. Available from: <URL>.

2. Ocsoy I, Dogru E, Usta S. A new generation of flowerlike horseradish peroxides as a nanobiocatalyst for superior enzymatic activity. Enzyme Microb Technol [Internet]. 2015 Jul;75–76:25–9. Available from: <URL>.

3. Hollmann F, Arends IWCE. Enzyme initiated radical polymerizations. Polymers [Internet]. 2012 Mar 6;4(1):759–93. Available from: <URL>.

4. Kalayci B, Kaplan N, Dadi S, Ocsoy I, Gokturk E. Production of flower-shaped nanobiocatalysts from green tea and investigation of their peroxidase mimicking activity on the polymerization of phenol derivatives. Polym Adv Technol [Internet]. 2024 Jan 13;35(1):e6272. Available from: <URL>.

5. Dordick JS, Marletta MA, Klibanov AM. Polymerization of phenols catalyzed by peroxidase in nonaqueous media. Biotechnol Bioeng [Internet]. 1987 Jul 18;30(1):31–6. Available from: <URL>.

6. Isci I, Gokturk E, Turac E, Sahmetlioglu E. Chemoenzymatic polymerization of hydrazone functionalized phenol. Polym Sci Ser B [Internet]. 2016 Jul 12;58(4):411–20. Available from: <URL>.

7. Kumbul A, Gokturk E, Turac E, Sahmetlioglu E. Enzymatic oxidative polymerization of para -imine functionalized phenol catalyzed by horseradish peroxidase. Polym Adv Technol [Internet]. 2015 Sep 4;26(9):1123–9. Available from: <URL>.

8. Ahmad R, Sardar M. Enzyme immobilization: An overview on nanoparticles as immobilization matrix. Biochem Anal Biochem [Internet]. 2015;4(2):1000178. Available from: <URL>.

9. Zhang Y, Ge J, Liu Z. Enhanced activity of immobilized or chemically modified enzymes. ACS Catal [Internet]. 2015 Aug 7;5(8):4503–13. Available from: <URL>.

10. Gupta MN, Mattiasson B. Unique applications of immobilized proteins in bioanalytical systems. In 1992. p. 1–34. Available from: <URL>.

11. Hanefeld U, Cao L, Magner E. Enzyme immobilisation: fundamentals and application. Chem Soc Rev [Internet]. 2013;42(15):6211–2. Available from: <URL>.

12. Ge J, Lei J, Zare RN. Protein–inorganic hybrid nanoflowers. Nat Nanotechnol [Internet]. 2012 Jul 3;7(7):428–32. Available from: <URL>.

13. Gokturk E, Ocsoy I, Turac E, Sahmetlioglu E. Horseradish peroxidase-based hybrid nanoflowers with enhanced catalytical activities for polymerization reactions of phenol derivatives. Polym Adv Technol [Internet]. 2020 Oct 4;31(10):2371–7. Available from: <URL>.

14. Ildiz N, Baldemir A, Altinkaynak C, Özdemir N, Yilmaz V, Ocsoy I. Self assembled snowball-like hybrid nanostructures comprising *Viburnum opulus L.* extract and metal ions for antimicrobial and catalytic applications. Enzyme Microb Technol [Internet]. 2017 Jul;102:60–6. Available from: <URL>.

15. Topal Y, Tapan S, Gokturk E, Sahmetlioglu E. Horseradish peroxidase-catalyzed polymerization of ortho-imino-phenol: Synthesis, characterization, thermal stability and electrochemical properties. J Saudi Chem Soc [Internet]. 2017 Sep;21(6):731–40. Available from: <URL>.

16. Oguchi T, Tawaki S ichiro, Uyama H, Kobayashi S. Soluble polyphenol. Macromol Rapid Commun [Internet]. 1999;20(7):401–3. Available from: <URL>.

17. Kumbul A, Gokturk E, Sahmetlioglu E. Synthesis, characterization, thermal stability and electrochemical properties of ortho-imine-functionalized oligophenol via enzymatic oxidative polycondensation. J Polym Res [Internet]. 2016 Mar 18;23(3):52. Available from: <URL>.

18. Kocak A, Kumbul A, Gokturk E, Sahmetlioglu E. Synthesis and characterization of imine-functionalized polyphenol via enzymatic oxidative polycondensation of a bisphenol derivative. Polym Bull [Internet]. 2016 Jan 4;73(1):163–77. Available from: <URL>.

19. Göktürk E. Flowerlike hybrid horseradish peroxidase nanobiocatalyst for the polymerization of guaiacol. TURKISH J Chem [Internet]. 2020 Oct 26;44(5):1285–92. Available from: <URL>.

20. Yildirim P, Gokturk E, Turac E, Demir HO, Sahmetlioglu E. Chemoenzymatic polycondensation of para-benzylamino phenol. Chem Pap [Internet]. 2016 Jan 30;70(5):610–9. Available from: <URL>.